

Innovative Multiple Matching Charts approach to support the conceptual design of hypersonic vehicles

Original

Innovative Multiple Matching Charts approach to support the conceptual design of hypersonic vehicles / Ferretto, D.; Fusaro, R.; Viola, N.. - In: PROCEEDINGS OF THE INSTITUTION OF MECHANICAL ENGINEERS. PART G, JOURNAL OF AEROSPACE ENGINEERING. - ISSN 0954-4100. - ELETTRONICO. - 234:12(2020), pp. 1893-1912. [10.1177/0954410020920037]

Availability:

This version is available at: 11583/2837731 since: 2020-09-22T14:39:39Z

Publisher:

SAGE Publications Ltd

Published

DOI:10.1177/0954410020920037

Terms of use:

This article is made available under terms and conditions as specified in the corresponding bibliographic description in the repository

Publisher copyright

Sage postprint/Author's Accepted Manuscript

Ferretto, D.; Fusaro, R.; Viola, N., Innovative Multiple Matching Charts approach to support the conceptual design of hypersonic vehicles, accepted for publication in PROCEEDINGS OF THE INSTITUTION OF MECHANICAL ENGINEERS. PART G, JOURNAL OF AEROSPACE ENGINEERING (234 12) pp. 1893-1912. © 2020 (Copyright Holder). DOI:10.1177/0954410020920037

(Article begins on next page)

Innovative Multiple Matching Charts approach to support the conceptual design of hypersonic vehicles

DAVIDE FERRETTO

*Department of Mechanical and Aerospace Engineering, Politecnico di Torino, Corso Duca degli Abruzzi, 24
10129, Turin, Italy*
davide.ferretto@polito.it

ROBERTA FUSARO

*Department of Mechanical and Aerospace Engineering, Politecnico di Torino, Corso Duca degli Abruzzi, 24
10129, Turin, Italy*
roberta.fusaro@polito.it

NICOLE VIOLA

*Department of Mechanical and Aerospace Engineering, Politecnico di Torino, Corso Duca degli Abruzzi, 24
10129, Turin, Italy*
nicole.viola@polito.it

Abstract

Several well-established best practices and reliable tools have been developed along the years to support aircraft conceptual and preliminary design. In this context, one of the most widely used tool is the Matching Chart, a graphical representation of the different performance requirements (curves representing the Thrust-to-Weight ratio requirement as function of the Wing Loading) for each mission phase. The exploitation of this tool allows the identification of a feasible design space as well as the definition of a reference vehicle configuration in terms of maximum thrust, Maximum Take-Off Weight and wing surface since the very beginning of the design process. Although the tool was originally developed for conventional aircraft, several extensions and updates of the mathematical models have been proposed over the years to widen its application to innovative configurations. Following this trend, this paper presents a further evolution of the Matching Chart model to support the conceptual design of high-speed transportation systems, encompassing supersonic and hypersonic flight vehicles. At this purpose, this paper reports and discusses the updates of the methodology laying behind the generation of the Matching Chart for high-speed transportation. Eventually, the results of the validation of the updated methodology and tool are reported, using as case study, the STRATOFLY MR3 vehicle configuration, a Mach 8 antipodal civil transportation system, currently under development within the H2020 STRATOFLY Project.

Keywords: High-speed transportation, Matching Chart, Aircraft Design, Conceptual Design methodology and tools

1. Introduction

The conceptual design phase aims at sketching the general layout of the aircraft, providing preliminary mass breakdown as well as the indication of the aircraft general performance starting from high-level requirements such as payload mass, maximum range, cruise speed and altitude, specific fuel consumption as well as operational aspects. The final goal of the conceptual design phase is the assessment of the feasibility of both the vehicle and the mission concept from the technical and operational standpoints. Many best practices and guidelines for aircraft conceptual design are available in literature [1-3], suggesting typical workflows to draft a vehicle configuration and to evaluate the impact of requirements on the vehicle's architecture and performance. In these processes, special attention is paid to the identification or development of tools able to depict the design space at a glance, meeting stakeholders' expectations with design feasibility criteria [4]. In this context, the proper definition of the basic performance (e.g. mass, thrust and lifting surface) of the vehicle is a crucial point for the selection of a plausible design point to be considered as the baseline for the next development phases. In 1980's NASA introduced a simple way of representing propulsion plant requirements matching with vehicle configuration within the so-called Matching Chart (MC) [5]. This is a graphical representation which relates thrust-to-weight ratio (T/W) to the wing loading (W/S) of the aircraft on a 2D chart (Fig. 1). This chart allows the identification of a feasible design space and the definition of a design point describing the optimal vehicle configuration in terms of Maximum Thrust, Maximum Take-Off Weight (MTOW) and wing surface, meeting all the high-level requirements. In the MC, the different curves or lines are mathematical equations that express each mission phase throughout its T/W request as function of the W/S . Practically speaking, it identifies a spectrum of feasible solutions, in terms of required thrust to counteracts the drag generated during the flight, with a direct correlation to the lift generation capability of the aircraft.

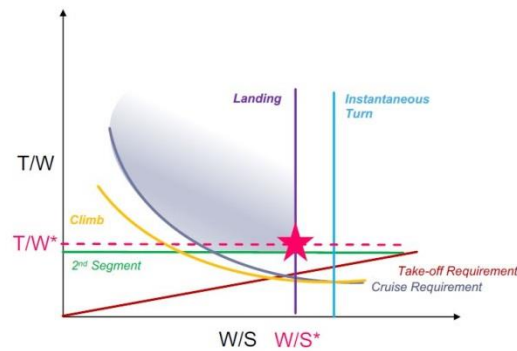


Fig. 1: Sketch of a typical Matching Chart

In the past, this approach, which provides a global overview of aircraft performance as preliminary assessment, has been exploited, for a wide range of case studies (conventional and innovative configuration, as well). At this purpose, updates and upgrades of the tool have been suggested to cope with a wider number of mission concepts and vehicle configurations [6]. Furthermore, in other cases, multi-dimensional or parametric analyses have been included to assess the reliability of the solutions [7,8].

In this context, this paper aims at further extending the current version of the MC methodology and tool to specifically manage the design of high-speed vehicles, providing updated and/or brand-new mathematical formulations to cope with the supersonic and hypersonic mission phases. The development of such a powerful tool, based on a rigorous methodology, will provide engineers with a valuable support to address the worldwide incentive to consider commercial high-speed transportation systems for both aeronautical and space applications. On one side, high-speed vehicles could be considered as the natural evolution of civil transportation while on the other side they could be seen as test-beds for enabling technologies for future reusable access to space and re-entry systems. Section 2 gives an overview of the way in which the MC methodology is currently exploited within a modern conceptual design workflow for conventional aircraft, and it highlights at the same time, the differences that may arise in case of hypersonic vehicle design. In this case, main differences are related to the adoption of highly sophisticated propulsive subsystems, characterized by very different modes of operations all along the mission. Then, Section 3 introduces the new mathematical models to update the matching chart methodology. Subsequently, Section 4 presents the application of the updated methodology and tool to the selected case-study, the STRATOFly MR3 vehicle configuration, currently under investigation within the H2020 STRATOFly Project [9]. Ultimately, conclusions are drawn in Section 5 together with ideas for future improvements.

2. Matching analysis and Matching Chart tool exploitation in Conceptual Design

2.1 Typical role of Matching Chart in Conceptual Design for subsonic aircraft

Subsonic vehicles are typically designed to meet high-level requirements generally related to payload, range, cruise specifications (i.e. Mach number and ceiling) as well as to airport performance, such as the take-off field length or balance field length, the landing distance, or missed approach and second segment climb gradient. These performance requirements have a direct impact on many physical characteristics of the aircraft, and thus on the vehicle size and mass breakdown. Fig. 2 summarizes the original activity flow leading to the generation of the Matching Chart (MC) [5]. The analysis starts from the definition of proper requirements concerning airport performance and cruise parameters to determine Thrust-to-Weight ratio and Wing Loading in the different flight conditions. In addition, data related to the aerodynamic characteristics of the aircraft in each mission phase, at least in terms of lift and drag coefficients shall be available at the beginning of the process. They can also serve as basis for a further parametric analysis to assess the impact of the hypothesized aerodynamic configuration of the aircraft onto the design space. The block called simultaneous solution (step 6 of the flow in Fig. 2) is the MC itself, which collects the different requirements expressed in terms of Thrust-to-Weight ratio (T/W) and wing loading (W/S) and defines a performance-oriented design space. Through the MC, it is possible to select specific values of T/W and W/S (step 7 of the flow-chart in Fig. 2) and thus, to select a single configuration to be used as baseline for further investigations. In particular, for each selected design point, it is possible to define a proper mass breakdown as well as to verify the consistency with the range requirement. Indeed, at this level, the mass breakdown encompasses payload mass, fuel and main subsystems mass as well as, ultimately, the maximum take-off mass. Complementary, the range equation, typically computed in conceptual design following the Breguet model [3], allows relating the performance of the propulsion plant, such as thrust and specific fuel consumption, to cruise data and fuel mass.

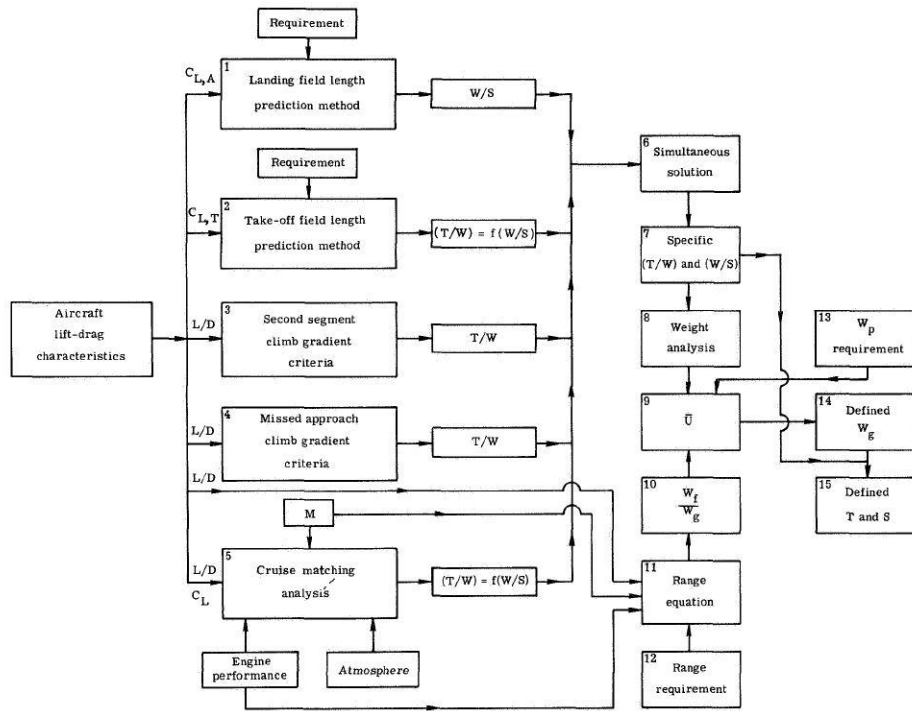


Fig. 2: Subsonic aircraft conceptual sizing process [5]

This aircraft sizing process allows evaluating the different flight conditions and propulsion subsystem performance in one-shot, since the engine can be characterized in terms of the performance that shall be achieved in all mission phases, working as a typical turbojet or turbofan. At the same time, the aerodynamics of the aircraft is characterized by looking at the most demanding flight regime. Therefore, the exploitation of MC tool during the conceptual design for conventional aircraft, allows a rapid identification of a single and consistent configuration.

Fig. 3 shows a typical example of MC for a jet aircraft as reported in [5]. The different requirements are depicted as curves on the graph, representing the required T/W as function of W/S for each flight phase. In particular, this example shows requirements for take-off and landing, missed approach, second segment and cruise. In order to be comparable, the different equations are corrected to represent equivalent trends at sea level. The feasible area of the design space can be identified as the part of the graph characterized by T/W higher than the most stringent requirement (in this case, the cruise) and with W/S lower than the most stringent requirement (in this case, the landing). In particular, the match point is located where the minimum T/W is reached, coupled with consistent W/S value. Usually, maximum W/S (i.e. minimum required wing surface) is selected, taking into account landing requirement for civil aircraft. On the contrary, in the case reported in Fig. 3 the take-off requirement is considered as the most critical, since a higher wing surface (i.e. a lower loading) is selected, thus giving priority to a lower T/W . The landing requirement would have led to the selection of a higher W/S with a higher T/W ratio, more demanding for the propulsion plant. This is a typical example of the introduction of additional constraints on power plant or specific needs of the stakeholders.

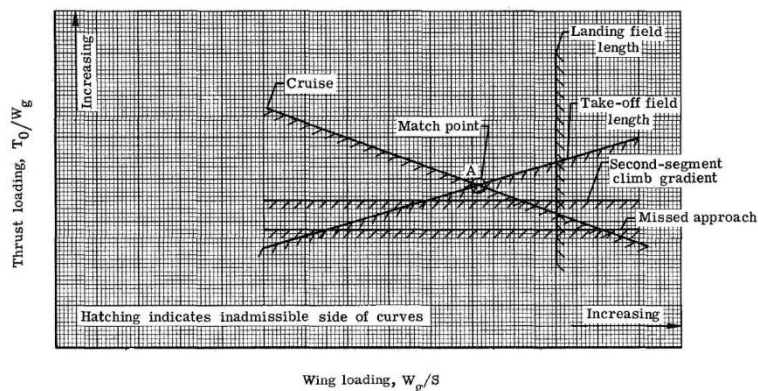


Fig. 3: Example of a typical Matching Chart for jet-powered aircraft [5]

2.2 Analogies and differences between subsonic and high-speed vehicles matching charts

Even if the Matching Chart (MC) provides the designer with a complete understanding of the design space for conventional and non-conventional aircraft during conceptual design, as discussed in Section 2.1, it cannot be applied as it is for the analysis of high-speed transportation systems that may be significantly different from conventional aircraft, especially in terms of mission profile and propulsion plant. In fact, on one side, the limits of application of the mathematical formulations for the already existing curves shall be extended to cover supersonic and hypersonic flight regimes. Complementary, the higher level of complexity, innovation and integration of the high-speed vehicles shall also be considered to develop a tool able to provide results with an acceptable confidence level. In particular, considering that one of the most important variables is the engine thrust, the update and upgrades of the MC shall consider the fact that these vehicles are often equipped with different propulsive subsystems to cover the wide spectrum of flight regimes and operative environments. The same considerations are applicable in case of the most recent combined cycle propulsive subsystems. Taking all these elements into account, it appears clear that a single MC is no more sufficient to represent the whole set of requirements and that a single design point can only describe a specific mode of operation of the propulsive subsystem. Reporting all the requirements coming from different speed regimes on the same design space within a unique diagram, may lead to wrong results and unfeasible solutions. For example, traditionally, the Thrust-to-Weight ratio (T/W) requirements are normalized using a specific altitude (e.g. sea level) to allow comparisons but this is no more applicable for high-speed transportation. Indeed, in the case of hypersonic transportation, the attempt to create a single MC representing several propulsive subsystems, operating at different altitudes, may lead to an overestimation of the T/W requirement (Fig. 4).

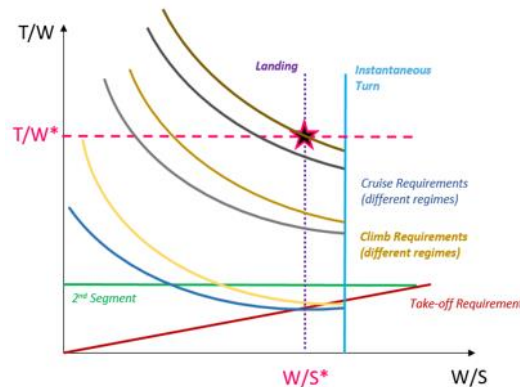


Fig. 4: Multi-regime, single Matching Chart approach

Indeed, the comparison between subsonic and hypersonic cruises requirements is not meaningful anymore, because in reality the two cruise legs are performed by different engines or even by the same engine but working in different modes of operations. Complementary, the normalization of the hypersonic cruise requirement using sea-level as reference atmospheric condition, would result in an extremely high required thrust.

Therefore, a Multiple Matching Charts (MMC) approach is here suggested to tackle the conceptual design of hypersonic vehicles. Basically, high-level requirements and performance assessment is carried out for each speed regime separately. However, a synthesis is necessary to guarantee the fulfilment of some physical and geometrical constraints. Indeed, even if the MMC brings the designers to define different scales to draw T/W requirements for the various flight regimes, this is not applicable for the Wing Loading (W/S) requirements. Indeed, even if T/W requirements may change all along the mission, the wing surface cannot. Thus, after the derivation of T/W requirements using the MMC approach, iterations shall be carried out to identify a unique value of wing surface able to generate a sufficient amount of lift to fulfil the requirements of the various flight regimes. The subsonic condition, and in particular the landing requirement, is expected to drive the selection of the unique design point, being the most demanding requirement (i.e. the widest wing surface). Of course, landing requirement curves are not present in the MC for supersonic or hypersonic regimes and the manoeuvres requirements in high speed flight are limited by passenger comfort and maximum structural loads, thus they require a lower wing surface. Local design points for subsonic, supersonic and hypersonic regimes would then be probably different in terms of required surface. Moreover, the selection of a suitable W/S at high speed is influenced by a lower vehicle mass, if compared to subsonic regimes (the propellant required to reach hypersonic cruise altitude has already been used during the acceleration phases). This means that, for example, it is not realistic to define the requirement for hypersonic cruise considering the Maximum Take-Off Weight (MTOW).

These different aspects contribute to define local design points for each regime (i.e. for each MC), identified by specific values of W/S and T/W . The consistency of the final solution shall be guaranteed, iterating the process up until all selected design points are characterized by the same wing surface (determined within the most critical flight regime) as well as by the reference mass of the considered phase. This means that an additional requirement is implicitly present in the chart, imposing the consistency among the different flight regimes in terms of W/S . Local (purple star) and global (green star) design points shall then be identified within the MMC depending on the number of flight regimes (Fig. 5), where the global solution identifies the point characterized by the W/S computed with the maximum required wing surface as well as by the highest T/W . The target value of thrust to be used for the sizing of the propulsion plant will then be the one corresponding to the value of W/S specified by the consistency requirement (most demanding condition). The exploitation of the MMC approach thus allows preventing the underestimation of thrust requirements in high-speed that might result from very small wing surface usually evaluated locally for the high-speed regime. At the same time, the value of thrust obtained using the MMC approach, is way more reasonable than the one computed with the traditional single chart methodology, affected by several errors related to wrong requirements normalization, to misleading propulsion plant operation and not consistent aircraft mass.

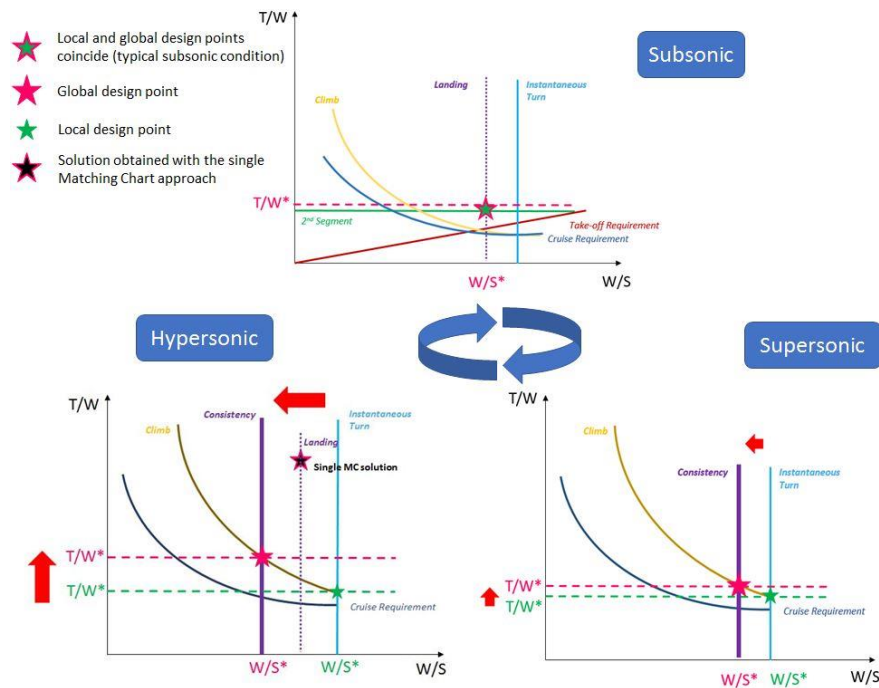


Fig. 5: Multi-regimes, multiple Matching Chart approach

From the sketch reported in Fig. 5 it is possible to notice the progress through the identification of the design points. In the subsonic case, global and local solutions usually coincide, since this is the most critical condition for the determination of wing surface. In supersonic a smaller number of requirements is present, but two solutions exist. In fact, the requirements for the pure supersonic regime provide a local design point determined by the combination of climb and manoeuvre. However, the consistency requirement determined by the configuration obtained in subsonic shall be satisfied, allowing the selection of a global design point characterized by a higher T/W and a lower W/S . Eventually, the progressive reduction of reference mass (from subsonic to hypersonic flight regime) produces a global design point in hypersonic which is even further from the local one if compared to the supersonic phase for similar reasons. Moreover, while focusing on the hypersonic MC, it is possible to see that the difference between this global design point and the one obtainable with the single MC approach (black star, typically located on the trace of subsonic landing requirement for that specific methodology) is usually non-negligible, both in terms of W/S and T/W . This is also due to the fact that the density correction (thrust normalization) cannot be performed directly considering sea level, as in the original MC methodology, whilst different reference altitudes shall be identified per each flight phase. This leads to the selection of proper cruise or top-of-climb altitudes for supersonic and hypersonic flight phases as reference to normalize the requirements. Taking all these considerations into account, the following set of upgrades shall be implemented to enhance the traditional MC methodology to deal with the conceptual design of high-speed vehicles:

- the process shall be able to include the presence of different propulsion subsystems or complex combined cycles engines, able to operate in a wide range of operating modes at various speed regimes leading to the generation of different MC;
- a wider spectrum of flight altitudes shall be considered to correctly set the chart, in conjunction with engines operations and flight phases, also implementing a complete atmospheric model covering the complete altitude range;
- new equations shall be included to represent requirements for additional flight regimes with respect to subsonic one;
- the analysis of the most critical conditions shall be assessed to identify proper vehicle configuration in terms of T/W ratio and W/S, verifying the matching for local and global design points. Notably, local design points will identify the matching of the aircraft in the specific flight regime, especially in terms of wing surface, while global matching will consist in a summary of most critical conditions, imposing a consistency requirement of aircraft geometrical configuration, and providing the final target value of T/W ratio to be used for the sizing of the propulsion plant.

Now, looking at each flight regime separately, the design loop here implemented (Fig. 6), and described in details in the following paragraphs, is similar to the original one depicted in Fig. 2.

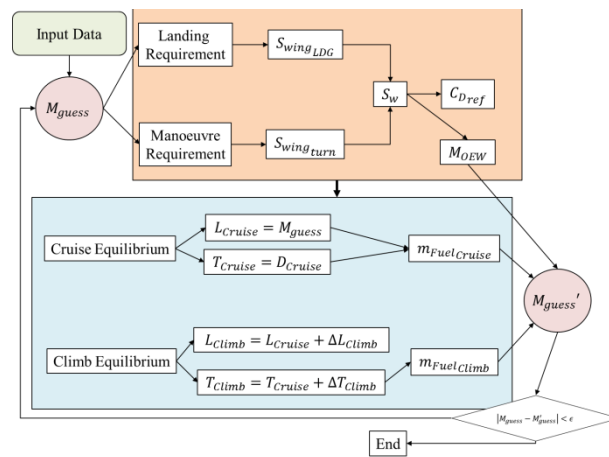


Fig. 6: General conceptual sizing process

In fact, starting from some basic input data concerning mission and high-level aircraft characteristics (configuration), as well as hypothetical power plant performance, it is possible to derive the minimum value of wing surface which guarantees enough lift in landing and manoeuvre conditions (Section 3). The reference value selected for subsequent steps is the most critical one, determining the Operating Empty Weight (OEW) and reference drag coefficients of the vehicle (Section 3). Typical Weight Estimation Relationships (WERS) are in fact based on wing surface and other aircraft parameters to estimate OEW, as reported in [7] and [10]. Moreover, by means of a simple set of well-known equilibrium conditions [3], it is possible to derive thrust and fuel mass required for the most significant phases of the mission. Fuel computation is relatively simple to obtain, once mission and vehicle configuration data are available, as reported by (1), following Breguet model [3]

$$M_{fuel} = M_{guess} \left(1 - e^{-\frac{R \cdot g \cdot SFC}{V \cdot L/D}} \right) \quad (1)$$

where:

M_{guess} is the overall mass of the vehicle as computed in the current iteration cycle [kg]

R is the range of the specified phase [m]

g is gravity acceleration $\left[\frac{m}{s^2} \right]$

SFC is Specific Fuel Consumption of the reference engine $\left[\frac{kg}{s \cdot N} \right]$

V is reference speed of the phase $\left[\frac{m}{s}\right]$

$\frac{L}{D}$ is aircraft aerodynamic efficiency

An updated value of vehicle mass can then be derived and compared to the guess data used at the beginning of the process. If the difference between the two values is within a specified range, the design loop is completed and the MC can be created, otherwise it is necessary to iterate the algorithm. The process converges since the increase of mass is limited, being reduced at each iteration. This is due to the fact that the equilibrium conditions produce an increase of lift generation capability (lift shall be equal to weight) that is always higher than the increase of drag determined by the growing of vehicle size, progressively converging on the correct amount of fuel required to cover the specified range.

The loop is valid for each flight regime covered within the MMC approach. However, an additional mass shall be considered for supersonic and subsonic cycles to account for the mass of fuel required for subsequent mission legs. In these cases, a proper fuel mass shall be included within the updated value of mass derived at the end of the cycle (notably reference mass for subsonic regime shall include fuel quantity necessary for supersonic and hypersonic conditions, whilst, as far as supersonic regime is concerned, the fuel required for hypersonic leg shall be considered as additional mass). Convergence is thus more complex in MMC than in single MC approach, since a double iterative loop structure is present to take into account local and global solutions.

In order to take a closer look to the curves populating the MC, Section 3 proposes a new mathematical model for the derivation of the requirements, while Section 4 provides an overview of the MMC sizing process, applying the aforementioned methodology to the STRATOFLY MR3 case study (Section 4.2). The results of the application of MMC-based design are then compared with the available data of the MR3 vehicle (Section 4.1), to validate the method.

3. Updates of the mathematical model of the Matching Chart for high-speed transportation systems

3.1. Introduction

Section 3 aims at proposing a new the mathematical model laying behind the generation of the requirements' curves populating a Matching Chart (MC), in terms of Thrust-to-Weight ratio (T/W) and wing loading (W/S) to widen its range of applicability to include high speed vehicles. The mathematical models here presented are described looking at the different flight phases separately, from Section 3.2 up to Section 3.12. In general, three types of relationships can be defined in the MC:

- Equations in which $T/W = f(W/S)$, such as take-off, climb, cruise and sustained turn requirements
- Equations which are characterized by $T/W = const$, such as second segment requirement
- Equations which are characterized by $W/S = const$, such as landing and instantaneous turn requirement

As final remark, a discussion on the possibility of including additional requirements in the MC is reported in Section 3.13, in order to analyse the possibility to enlarge the MC concept and to enhance the derivation of the design point.

3.2. Take-off distance requirement

The take-off phase is usually defined as the sequence of run, rotation (or manoeuvre) and climb segments which brings the aircraft from ground up to 35 ft of altitude with reference to ground elevation. The overall horizontal distance travelled during the whole phase is known as take-off field length, while the distance required for the aircraft to leave the ground is called lift-off distance (corresponding basically to run segment). In general, MC requirements are usually referring to this specific parameter, even if usually addressed as take-off distance. To maintain consistency with literature, the same concept is here adopted.

The simplified derivation of the lift-off distance requirements is derived, making the hypothesis that the aerodynamic drag on ground can be neglected as well as the rolling friction between the wheels and the runway. The following constitutive equations are then applied: Eq. (2) defines the run to lift-off l_{LO} , Eq. (3) represents the equilibrium condition and Eq. (4) identifies the lift-off speed V_{LO} .

$$l_{LO} = \frac{V_{LO}^2}{2a_{LO}} \quad (2)$$

$$\frac{T_{LO}}{W_{LO}} = \frac{a_{LO}}{g} \quad (3)$$

$$V_{LO} = \sqrt{\frac{W_{LO_{kg}} g}{\frac{S C_{L_{LO}} \rho}{2}}} \quad (4)$$

Where:

a_{LO} is the acceleration at lift-off in $\frac{m}{s^2}$

T_{LO} is the thrust generated by the propulsion plant at lift-off in N

W_{LO} is the aircraft weight at lift-off in N

$W_{LO_{kg}}$ is the aircraft mass at lift-off in kg

S is the wing surface of the aircraft in m^2

ρ is reference air density in $\frac{kg}{m^3}$

$C_{L_{LO}}$ is the lift coefficient at lift-off

By combining the constitutive equations it is possible to express the lift-off distance, i.e. take-off run (5), in terms of W/S and T/W .

$$l_{LO} = \frac{W_{LO_{kg}}/S}{T_{LO}/W_{LO} C_{L_{LO}} \rho_0 \sigma} \quad (5)$$

Where:

$\sigma = \rho/\rho_0$ is the density ratio between reference air density and sea level density

Eventually, the take-off distance requirements can then be defined as in (6), simply re-arranging Eq. (5).

$$\left(\frac{T}{W}\right)_{LO} = \frac{W_{LO_{kg}}/S}{\rho_0 \sigma l_{LO} C_{L_{LO}}} \quad (6)$$

3.3. Second segment requirement

The second segment is the portion of flight path during take-off starting from gear-up altitude (after the 35 ft obstacle) and ending at 400 ft minimum. Applicable regulations for conventional aircraft [10] define the phase and provide some details regarding reference speed and climb gradient to be guaranteed in case of engine failure as follows:

- Flight speed is constant and equal to V_2
- Minimum climb gradient G_{2nd} to be guaranteed in case of multiple engines configuration is equal to
 - 2.4% in case of two engines
 - 2.7% in case of three engines
 - 3.0% in case of four engines

Since there is neither a specification for more than four engines, nor even suggestions for high speed transportation systems, the most strict requirement coming from [10] is adopted. The following constitutive equation (7) can be used:

$$\left(\frac{T}{W}\right)_{2nd} = \left(\frac{D}{W}\right)_{2nd} + G_{2nd} \quad (7)$$

where

$\left(\frac{T}{W}\right)_{2nd}$ is the Thrust-to-Weight ratio in second segment

$\left(\frac{D}{W}\right)_{2nd}$ is Drag-to-Weight ratio in second segment

Considering that, as preliminary assumption, lift shall compensate the weight in all conditions and that the climb gradient G_{2nd} shall be guaranteed also in case of One Engine Inoperative (OEI) scenario, second segment requirement (8) can be derived starting from (7):

$$\left(\frac{T}{W}\right)_{2nd} = \frac{N_{engines}}{N_{engines} - 1} \left(\frac{1}{E_{2nd}} + G_{2nd} \right) 1/\sigma \quad (8)$$

where

E_{2nd} is the aerodynamic efficiency in second segment

As it can be seen from (8) this requirement is not a function of wing loading.

3.4. Subsonic climb requirement

The subsonic climb requirement can be simply derived following the traditional approach that consists in using the equation of the quadratic polar theory to define drag as in (9):

$$D = C_{D0} + kC_L^2 \quad (9)$$

where

C_{D0} is the drag coefficient at zero lift

C_L is the lift coefficient

$k = \frac{1}{\pi A e}$ where A is the aspect ratio and e is the Oswald factor

Moreover, the contribution of the second term of (9), representing the induced drag, is usually neglected as preliminary assumption. Drag can then be computed as in (10):

$$D \approx q_\infty S C_{D0} \quad (10)$$

where

q_∞ is the dynamic pressure of the incoming flow in Pa

For this specific flight regime, the computation of C_{D0} is performed using subsonic drag component build up [3] as specified in (11).

$$(C_{D0})_{subsonic} \approx \frac{\sum C_f F_F Q S_{wet}}{S_{ref}} \quad (11)$$

where

C_f is the skin-friction drag coefficient

F_F is the form factor of selected component (fuselage, wing, tail etc...) that estimates pressure losses due to viscous separation

Q is the interface factor for the selected component

S_{wet} and S_{ref} are the wetted surface for the selected component and the reference wing surface respectively expressed in m^2

In equation (11), the contributions for miscellaneous as well as leakages and protuberances drag which are typically included in the build-up process are neglected.

Considering that the T/W can be expressed in a similar way with respect to (7), the subsonic climb requirement can be derived as in (12):

$$\left(\frac{T}{W}\right)_{subclimb} = \left(\frac{q_\infty C_{D0}}{W_{kg}/S g} + G_{subclimb} \right) \frac{1}{\pi\sigma} \quad (12)$$

where

$G_{subclimb}$ is the subsonic climb gradient

π is the throttle

This requirement is usually corrected using density ratio σ in order to be consistent with sea-level conditions. Moreover, throttle is used to evaluate the required T/W increase in case of flight at throttle level less than 100% for fuel saving purposes.

3.5. Subsonic cruise requirement

The model for subsonic cruise is similar to the one proposed in Section 3.4 for the subsonic climb. However, in this case, the climb gradient is neglected since the aircraft shall maintain its altitude. Preliminary assumptions used in (9) and (11) still apply, even if additional details shall be included in order to take into account the type of cruise considered. In fact, even if for hypersonic vehicles the subsonic cruise is supposed to be just an intermediate phase in the mission profile, it is still possible to distinguish between best range (13) and best endurance (14) [3] for the computation of the drag coefficient.

$$C_{D_{BR}} = \frac{4}{3} C_{D_0} \quad (13)$$

$$C_{D_{BE}} = 2C_{D_0} \quad (14)$$

This leads to the definition of subsonic cruise requirements to be used within the MC as in (15) and (16).

$$\left(\frac{T}{W}\right)_{subcruise_{BR}} = \left(\frac{q_\infty S \frac{4}{3} C_{D_0}}{W_{kg}/S g}\right) \frac{1}{\pi \sigma} \quad (15)$$

$$\left(\frac{T}{W}\right)_{subcruise_{BE}} = \left(\frac{q_\infty S 2 C_{D_0}}{W_{kg}/S g}\right) \frac{1}{\pi \sigma} \quad (16)$$

3.6. Supersonic climb requirement

The model for supersonic climb is again very similar to the one used for subsonic climb, even if the drag coefficient is computed in different way. The climb equilibrium equation is the same of (7) even if with a different climb gradient $G_{superclimb}$ but the drag coefficient for zero lift can be computed as in (17).

$$(C_{D_0_{supersonic}}) \approx \frac{\sum C_f S_{wet}}{S_{ref}} + C_{D_{wave}} \quad (17)$$

As it can be seen from (17), the contributions of form and interface factors is not included in the supersonic formulation. Moreover, as for (11), contributions for miscellaneous as well as leakages and protuberances drag, which are typically included in the build-up process, is here neglected. The contribution of wave drag is instead included referring to the equivalent Sears-Haack body characterized by the same length and total volume [3].

Eventually, the supersonic climb requirement can be derived as in (18).

$$\left(\frac{T}{W}\right)_{superclimb} = \left(\frac{q_\infty C_{D_{supersonic}}}{W_{kg}/S g} + G_{superclimb}\right) \frac{1}{\pi \sigma^*} \quad (18)$$

The correction with reference density in this case can be different depending on the configuration of the propulsion plant. σ^* can then be adapted looking at Top Of Climb (TOC), Bottom (or Beginning) of Climb (BOC) or other reference altitude.

3.7. Supersonic cruise requirement

The supersonic cruise requirement can be derived as already done for supersonic climb requirement in Section 3.6 neglecting climb gradient. It is then straightforward to derive the equation for the requirement reported in (19).

$$\left(\frac{T}{W}\right)_{\text{supercruise}} = \left(\frac{q_{\infty} C_{D_{\text{supersonic}}}}{W_{kg}/S g}\right) \frac{1}{\pi \sigma^*} \quad (19)$$

Similar considerations concerning σ^* applies also for supersonic cruise.

3.8. Hypersonic climb requirement

The derivation of proper requirements for the hypersonic phases are quite different from those of the other flight regimes since the physical models representing these conditions are no more applicable. After a review of the available models describing the behavior of the vehicle in hypersonic flight regime, the Newton theory has been selected [12, 13]. This approach allows to evaluate the aerodynamic characteristics for simplified geometrical shapes by relating pressure coefficients to the vehicle flight attitude that determines the external flow conditions. In particular, the scenario can be described by means of the angle of attack α , angle of the oblique shock β and angle characteristic of the body θ (such as leading edges angle etc...). In this case, the drag coefficient can be defined as in (20) for preliminary assumptions.

$$C_{D_{\text{hypersonic}}} = C_{p_{\text{Newton}}} \sin \alpha \quad (20)$$

Where pressure coefficient can be computed as in (21)

$$C_{p_{\text{Newton}}} = 2(\sin \theta)^2 \quad (21)$$

Apart from the form of drag coefficient equation, the hypersonic climb requirement is then similar to the one specified for previous climb segments (as described in Sections 3.6 and 3.4). The T/W requirement in hypersonic climb is then reported in (22).

$$\left(\frac{T}{W}\right)_{\text{hyperclimb}} = \left(\frac{q_{\infty} C_{D_{\text{hypersonic}}} + G_{\text{hyperclimb}}}{W_{kg}/S g}\right) \frac{1}{\pi \sigma^*} \quad (22)$$

3.9. Hypersonic cruise requirement

Similar assumptions apply also to hypersonic cruise requirement, that can be derived looking at the model used for hypersonic climb, neglecting climb gradient term. The result is reported in (23).

$$\left(\frac{T}{W}\right)_{\text{hypercruise}} = \left(\frac{q_{\infty} C_{D_{\text{hypersonic}}}}{W_{kg}/S g}\right) \frac{1}{\pi \sigma^*} \quad (23)$$

3.10. Instantaneous turn requirement

Instantaneous turn is a typical specification for military aircraft, such as fighters and trainers. It is a high performance index allowing the evaluation of the maneuverability. However, this requirement can also be included in the MC for other types of flight vehicles since the maximum load factor during the turn can be an index for structural integrity, identifying a proper level of wing loading associated to the maneuver. In fact, the turn rate can be determined as in (24)

$$\dot{\psi} = \frac{g\sqrt{n^2 - 1}}{V} \quad (24)$$

where

n is the load factor of the maneuver

Equation (24) has a simple physical interpretation, provided that n equal to one is required to sustain the aircraft, while the remaining load can be used to accelerate the vehicle on the horizontal plane on a circular trajectory. With this in mind, it is possible to express the load factor as in (25)

$$n = \frac{q_{\infty} C_L}{W_{kg}/S g} \quad (25)$$

Subsequently, the instantaneous turn requirement can be derived in terms of wing loading as in (26). Thus, this is not a requirement impacting on T/W, being represented as a vertical line on the MC.

$$\left(\frac{W_{kg}}{S}\right)_{IT} = \left(\frac{q_{\infty} C_{LMAX}}{ng}\right) \frac{1}{\sigma} \quad (26)$$

The instantaneous turn requirement uses the maximum lift coefficient in order to represent the maximum maneuver condition, consistent with maximum structural capability. Moreover, the density correction can be usually referred to sea level conditions, since the most of high load maneuvers are performed at low speed, in subsonic conditions. For other flight regimes, if this is the case, σ can be substituted with σ^* if a different reference altitude is used.

3.11. Sustained turn requirement

Sustained turn is defined as a turn performed at constant altitude and speed. This is, similarly to the case of the instantaneous turn, a typical requirement for fighter aircraft, for which it may be important to perform high performance maneuver during dogfight without losing speed. This requirement is here included as additional way to consider maneuvers close to minimum speed for hypersonic aircraft when flying at subsonic speed. The lift coefficient for the turn can be derived making equation (25) explicit. Moreover, since in the equilibrium during the turn the thrust shall compensate the drag, equation (27) can be derived.

$$T = q_{\infty} S C_{D_0} + q_{\infty} S k C_L^2 = q_{\infty} S C_{D_0} + \frac{n^2 W_{kg}^2}{q_{\infty} S k} \quad (27)$$

The sustained turn requirement can then be derived by making explicit equation (27), as shown in (28).

$$\left(\frac{T}{W}\right)_{ST} = \left(\frac{q_{\infty} C_{D_0}}{W_{kg}/S g}\right) \frac{1}{\sigma} + \left(\frac{W_{kg}}{S} g \left(\frac{n^2}{q_{\infty} \pi A e}\right)\right) \sigma \quad (28)$$

As for instantaneous turn, density ratio σ refers to sea level conditions.

3.12. Landing requirement

Landing requirement is important for commercial aircraft since it generally determines wing surface extension and related wing loading. The requirement is in fact a simple threshold for the wing loading in landing conditions, being as for the instantaneous turn, a vertical line on the MC. The landing model used for this work comes from the Loftin statistics [5] which is based on the evaluation of some semi-empirical parameters for jet-engine landing phase. Moreover, prescriptions from regulation [10] are applied to compute reference landing speed in non-icing conditions. In general, starting from the available landing distance s_{ALD} it is possible to compute the landing field length s_{LFL} as specified by (29).

$$s_{LFL} = 1.6 s_{ALD} \quad (29)$$

Where $s_{ALD} = \frac{v_{app}^2}{k_{app}^2}$ is the available landing distance obtained by dividing the approach speed by the approach parameter specified as $k_{app} = 1.7 \sqrt{\frac{m}{s^2}}$ in Loftin model.

Looking at landing equilibrium, it is possible to derive equation (30).

$$\frac{W_{kg}}{S} = \frac{\rho V_{ldg}^2}{2g} C_{LMAX} = \frac{1.23\rho_0\sigma C_{LMAX} k_{app}^2 S_{LFL}}{2g} \quad (30)$$

Equation (30) can be re-arranged to obtain a simple format as shown in (31).

$$\frac{W_{kg}}{S} = k_L \sigma C_{LMAX} S_{LFL} \quad (31)$$

Where

k_L is the Loftin parameter in $\frac{kg}{m^3}$

The shape of landing requirement can then be different depending on the actual configuration of the aircraft. In fact, it is possible to express wing loading at landing with both typical landing mass or higher. The selection of landing mass has in fact a considerable impact on the size of the wing and it is also influenced by regulatory aspect in case landing is required right after take-off in case of non-nominal conditions. Generally, it is possible to indicate two different landing requirements, as indicated in (32) and (33).

$$\left(\frac{W_{MLW_{kg}}}{S} \right)_{LDG1} = k_L \sigma C_{LMAX} S_{LFL} \quad (32)$$

$$\left(\frac{W_{MTOW_{kg}}}{S} \right)_{LDG2} = \frac{k_L \sigma C_{LMAX} S_{LFL}}{W_{MLW_{kg}} / W_{MTOW_{kg}}} \quad (33)$$

The first requirement is derived for Maximum Landing Weight (MLW) for which a specific landing mass is selected. The second requirement is instead fictional and referred to Maximum Take-Off Weight (MTOW) as main design mass. This second condition does not represent the normal landing condition, but it can be used to specify additional requirements on structural capability. Both wing loadings use the same reference surface.

3.13. Other requirements

Since the original approach, the MC gathers vehicle performance requirements related to the mission profile (altitude and Mach number of main phases, g-loads, rates of climb, landing and take-off field lengths). However, it is theoretically possible to include other families of high-level requirements within the MC representation, with the aim of extending this view towards high-level considerations affecting the conceptual design scenario. Indeed, specific constraints associated to fuel consumption, pollutant emissions, cost, safety as well as certification issues can be translated into proper requirements to be included within the chart. This would provide the designers with a broader understanding of the overall System of Systems in which the vehicle shall be able to operate, offering the possibility of selecting a more suitable design point, which can be generally different from the one derived by looking at mere performance drivers.

In this paragraph, some examples of the integration of additional requirements related to cruise time and fuel consumption are reported and overlapped to those previously defined for hypersonic regime of the case study, offering an interesting starting point for discussion. In fact, the requirements associated to climb and cruise phases (as depicted in Fig. 10 and Fig. 11 of Section 4.2), especially those representing the high-speed regimes, are defined starting from a fixed preliminary mission profile sketch. It is therefore interesting to evaluate the impact on the modification of phase legs and times on the design point as well as the effects of fuel consumption constraints. For example, an additional acceleration to be performed in cruise in case of reduction of initial speed (due to constraints on fuel consumption and pollutant emission on previous mission legs or justified by the need of keeping flight speed under a certain threshold over determined overflown areas) would define an additional requirement as in (34). At the same time, a proper constraint directly specifying fuel consumption limit can be defined as in (35), where fuel mass threshold is derived considering both maximum T/W and Specific Fuel Consumption (SFC) of the engine.

$$\left(\frac{T}{W} \right)_{hypercruise_{v0}} = \frac{D_{hypercruise} + W_{hypercruise_{kg}} a_{hypercruise}}{g W_{hypercruise_{kg}}} \quad (34)$$

$$\left(\frac{T}{W}\right)_{\text{hypercruise}_{FF}} = \frac{\dot{m}_F}{gW_{\text{hypercruise}_{kg}}SFC} \quad (35)$$

Where

$D_{\text{hypercruise}}$ is the aerodynamic drag in hypersonic cruise to be balanced by engine thrust in baseline condition [N]

$a_{\text{hypercruise}}$ is the required acceleration to reach cruise speed, considering a selected initial speed value $\left[\frac{m}{s^2}\right]$

\dot{m}_F is the maximum allowable fuel flow in hypersonic cruise $\left[\frac{kg}{s}\right]$

The requirement specified in (34) has an impact on cruise time, i.e. on overall mission time. This can be an interesting driver to select the proper mission scenario, taking into account passengers time value, economic feasibility and desirability with reference to conventional flights. The requirement on fuel consumption (35) is instead mainly related to cost and pollutant emission, which shall be kept under control. Actually, both requirements can be related to aircraft Direct Operating Cost (DOC), not only because they have a direct impact on fuel consumption during flight, but also since they can influence a lot the ticket price of the flight, as main consequence. Moreover, they can also be related to environmental issues concerning pollutant emissions of NOx and water vapor in flight, as well as of CO2 and other chemical species on ground during propellant production process. LH2 cost is in fact the main challenging aspect of the design-to-cost of this kind of vehicles, since the impact of propellant on overall DOC can be estimated about 70% of the total [14]. Moreover, a higher propellant mass fraction required per flight would have impact on the required production rate of LH2, i.e. on cost and on overall pollutant emissions within the vehicle fleet lifecycle. Actually, even if the increase in production rate may allow a reduction of the cost of LH2 per unit mass, as demonstrated in [15], the selection of cheap production process may still influence a lot the carbon footprint of the vehicle, even if the direct pollutant emissions in operation are strongly reduced. Moreover, requirement (35) brings also a technology level as driver in the design process. In fact, the SFC of the engine is a direct measure of the quality and efficiency of the power plant, being theoretically linked to the Technology Readiness Level (TRL) of propulsion systems, whose characteristics may influence a lot the design in case a specific entry-into-service estimate is available.

Moreover, modifications to the mission profile because of certification needs can be included within the requirements already defined in previous paragraphs. In fact, a part from maximum allowable g-loads requirements to limit passengers stress in hypersonic flight (already accounted in turns and maneuvers requirements), typical regulation concerns are associated to descent and landing phases of this kind of vehicles, usually designed to perform a gliding approach to ground. Proper requirements for missed approach or go-around procedures can be thus included within the MC, to take into account non-nominal scenarios. This would also bring in the game the key compromise between safety and cost, since a powered descent and landing would increase the possibility of react to emergency, while increasing the operating costs because of additional fuel required. Ultimately, Aircraft Traffic Management (ATM) issues cannot be forgotten, since gliding trajectories may require priority, with direct impact on the whole real time routes management, especially in the vicinity of airports.

Eventually, the MC approach offers many possibilities and an effective integration within the conceptual design process. In order to show examples of additional requirements and of their influence of the design space, equations (34) and (35) are included in Section 4.2 to analyze and discuss the design point change with respect to a performance-driven MC.

4. Matching of a Mach 8 hypersonic aircraft for passengers transportation

4.1. Case study: STRATOFLY MR3 hypersonic cruiser

As demonstrated in many studies carried out in the European framework over the last two decades, some innovative high-speed aircraft configurations have now the potential to assure an economically viable high-speed aircraft fleet. Investigations carried out in a succession of EC-supported research projects have permitted maturing a number of configurations leading to the airframe-integrated propulsion concept: ATLLAS I/II [16], LAPCAT I/II [17], HIKARI [18], HEXAFLY [19], HEXAFLY Int. [20]. They make use of unexploited flight routes in the stratosphere, offering a solution to the presently congested flight paths while ensuring a minimum environmental impact in terms of emitted noise and green-house gasses, particularly during stratospheric cruise. Only a dedicated multi-disciplinary integrated design approach could realize this, by considering airframe architectures embedding the propulsion systems, as well as meticulously integrating crucial subsystems. In this context, starting from an in-depth investigation of the current status of the activities, the STRATOFLY project has been funded by the European Commission, under the framework of Horizon 2020 plan, with the aim of

assessing the potential of this type of high-speed transport vehicle to reach TRL6 by 2035, with respect to key technological, societal and economical aspects. Main issues are related to thermal and structural integrity, low-emissions combined propulsion cycles, subsystems design and integration, including smart energy management, environmental aspects impacting climate change, noise emissions and social acceptance, and economic viability accounting for safety and human factors. The STRATOFLY MR3 vehicle configuration is currently under development (Fig. 7). This vehicle shall be capable of flying at Mach 8 in cruise at an altitude of 30 – 35 km carrying 300 passengers over antipodal routes (>18000 km range). The vehicle uses a dual propulsion plant based on air-breathing engines composed by six Air Turbo Rocket (ATR), to power the vehicle up to Mach 4.5, working as turbo rocket in subsonic condition and as ramjet in supersonic regime, and one Dual Mode Ramjet (DMR) which is ignited in hypersonic and works initially as ramjet, switching then to scramjet mode up to Mach 8. Engines used liquid hydrogen as propellant.



Fig. 7: STRATOFLY MR3 vehicle

Overall vehicle characteristics are reported in Table I.

Table I. STRATOFLY MR3 aircraft specifications

Parameter	Value	Unit of Measure
Length	94	<i>m</i>
Wingspan	41	<i>m</i>
Wing surface	1365	<i>m</i> ²
Aspect ratio	~1	-
MTOW	400000	<i>kg</i>
OEW	190000	<i>kg</i>
Payload (300 pax @ 100 kg)	30000	<i>kg</i>
Fuel Capacity	180000	<i>kg</i>
Cruise Mach	8	-
Service Ceiling	35000	<i>m</i>
Range	18700	<i>km</i>
ATR engines thrust @ sea level (total)	3000	<i>kN</i>
ATR engine thrust @ BOC supersonic (total)	2800	<i>kN</i>
DMR engine thrust @ BOC hypersonic	500	<i>kN</i>
DMR engine thrust @ hypersonic cruise level	1033	<i>kN</i>

The original vehicle concept, as well as reference mission Brussels – Sydney, were conceived within the EC funded project LAPCAT II [21] and detailed in STRATOFLY. The original mission adopted for this work is represented in Fig. 8. The mission comprehends the whole set of phases presented in Section 3 since, after take-off, the aircraft flies through subsonic climb and cruise, supersonic climb, supersonic cruise with ignition of DMR and switch-off of the ATR engines, hypersonic climb and cruise.

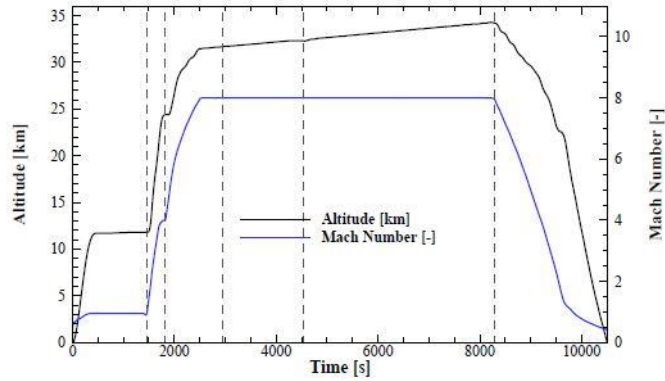


Fig. 8: Reference mission [21]

4.2. Matching analysis of STRATOFly MR3

The study here proposed aims at obtaining an aircraft sizing (mass estimation and vehicle matching) consistent with the original MR3 vehicle, keeping the high-level requirements of STRATOFly concerning Mach number, range, payload and ceiling, to demonstrate the effectiveness of the method. As comparison, the multi-regimes single Matching Chart (MC) approach is also provided at the end of this section (Fig. 14) to show the magnitude of the error related to the estimation of T/W in case of simultaneous matching of all conditions in a single chart. MR3 characteristics shown in Section 4.1 are used as reference to validate the results coming from the MMC analysis.

The MC for subsonic flight regime is shown in Fig. 9 for the converged solution. The requirements are corrected referring to sea level conditions. The landing requirement determines the wing loading (considering MTOW, solid red line, as reported in Table VI), whilst the maximum T/W is obtained for subsonic climb condition. With the low-speed configuration of the ATR engines, the propulsion plant is able to provide the required thrust in all conditions (the same available thrust levels of Table I are kept for consistency). Table II summarizes the design point for subsonic regime.

Table II: Design point for subsonic regime

Parameter	Value	Unit of measure
Wing loading (subsonic)	331	$\frac{kg}{m^2}$
Thrust-to-Weight ratio (subsonic)	0.783	-

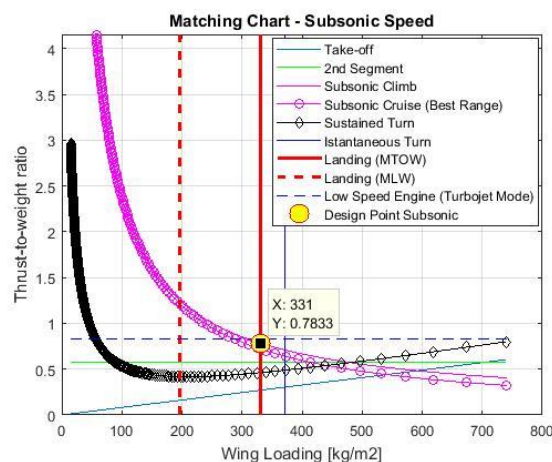


Fig. 9: Aircraft matching in subsonic flight

The Matching Chart for the supersonic regime is reported in Fig. 10. Please, notice that the diagram is corrected to show all trends with reference to the supersonic BOC, at 12000 m. For the supersonic flight regime, only climb and cruise requirements are included. Instantaneous turn is used to evaluate a possible wing loading to be used as reference for local design point. The turn is here hypothesized to generate a maximum acceleration load

on passenger cabin of about 0.3g (relative acceleration). The additional vertical red line (consistency requirement, as defined in Section 2.2) reports the W/S derived using the surface determined for subsonic condition with the aircraft mass at BOC supersonic. This allows representing a more realistic situation for the global design point in supersonic conditions, assuring a good estimation for the required T/W with respect to the local solution. For comparison purpose, both ATR and DMR thrust levels of the MR3 vehicle are shown, since a reduced contribution to the total thrust can be provided by the latter even outside its operating conditions, as demonstrated in [22]. In any case, the ATR engines in ramjet configuration are able to assure aero-propulsive balance of the vehicle without accounting the DMR. The summary of global design point coordinates in supersonic regime is provided in Table III.

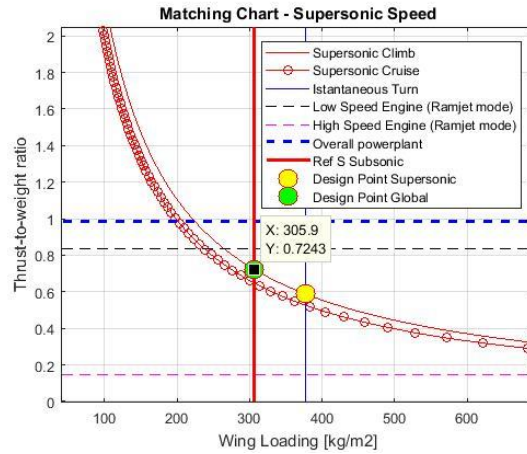


Fig. 10: Aircraft matching in supersonic regime

Table III: Global design point for supersonic regime

Parameter	Value	Unit of measure
Wing loading (supersonic)	305.9	$\frac{kg}{m^2}$
Thrust-to-Weight ratio (supersonic)	0.724	-

The Matching Chart for hypersonic regime is shown in Fig. 11. The diagram is corrected to show all trends with reference to the hypersonic BOC, at 24000 m.

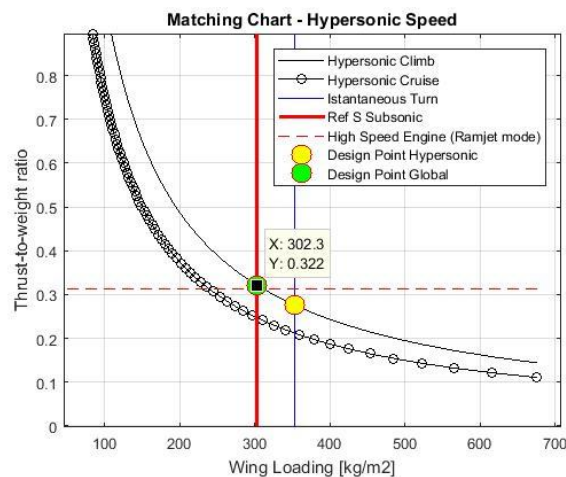


Fig. 11: Aircraft matching in hypersonic regime

As for the supersonic regime, only hypersonic climb and cruise are included. The instantaneous turn requirement is conceived in similar way to what already applied for the supersonic case. Moreover, the additional consistency requirements (red line in Fig. 11), positioned further on the left side and derived using subsonic wing surface and aircraft mass at hypersonic BOC, suggests the need for a higher thrust required. In fact, the available T/W is not

totally sufficient to support the aircraft in hypersonic cruise, since the DMR thrust seems to be too low. Table IV summarizes the coordinates for global design point in hypersonic conditions.

Table IV: Global design point for hypersonic flight regime

Parameter	Value	Unit of measure
Wing loading (hypersonic)	302.3	$\frac{kg}{m^2}$
Thrust-to-Weight ratio (hypersonic)	0.322	-

It is also interesting to evaluate the effect of the requirements specified in Section 3.13 on the hypersonic regime design space. Particularly, requirements on initial speed and on maximum fuel flow in hypersonic cruise are reported in Fig. 12. In this case, a modified mission profile with initial hypersonic cruise Mach equal to 5 is considered, together with a maximum fuel flow in the same phase of 20 kg/s.

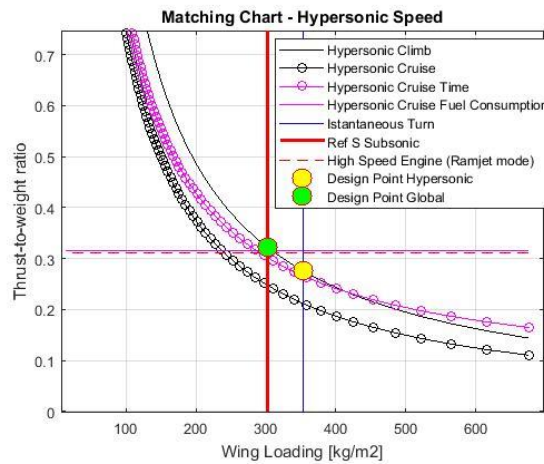


Fig. 12: Aircraft matching in hypersonic regime with additional requirements

As it is reasonable to expect, the design point is not very much influenced by the additional requirements, since the engine is compliant with fuel flow constraint and climb requirement is still more critical than the one associated to cruise acceleration. However, it is interesting to discuss the impact of new requirements on the feasibility design space. Looking closer to the region near the design points (Fig. 13) it is possible to identify different areas.

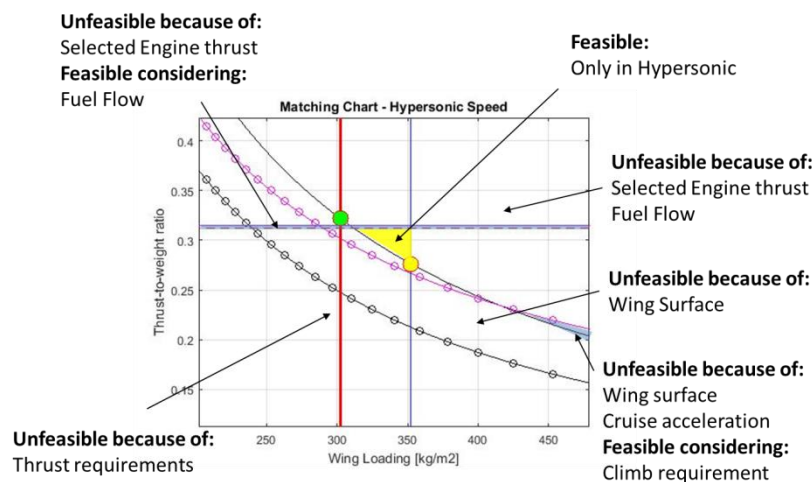


Fig. 13: Identification of feasibility space in presence of different kinds of requirements

It is clear that, starting from the baseline configuration, the global design point is already slightly above the available engine thrust threshold, thus the solution appears unfeasible (wing loading requirement is low because wing surface is constrained by landing requirement in subsonic regime). However, it is interesting to look at hypersonic regime requirements only, to discuss the inclusion of additional specifications (Section 3.13). The

superimposition of different families of requirements identifies a small feasibility region (yellow triangle in Fig. 13), where all statements are satisfied, considering a wing loading requirement uniquely valid in hypersonic regime. Other areas are unfeasible for multiple reasons, whilst specifications coming from Section 3.13 do not modify very much the design space. It is notwithstanding possible to locate areas characterized by conflicting needs (light blue areas in Fig. 13), where either performance requirements are satisfied and operational constraints are not, or vice-versa. This result allows understanding that high-level requirements related to the overall design scenario may be crucial to correctly estimate the feasibility space since they may reduce the design area, which is already intrinsically tight because of demanding performance requirements. Ultimately, in order to provide a mean of comparison between the results obtained with the proposed approach and those derived with the single MC methodology, Fig. 14 shows the equivalent design point for the vehicle in the single design space (only with performance requirements).

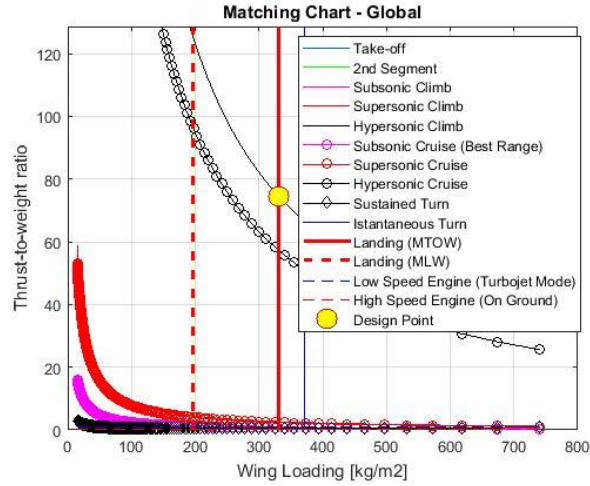


Fig. 14: Design point (unrealistic) obtained through the single Matching Chart approach for the MR3 vehicle

As it can be seen, the hypersonic climb requirement is setting a design point in terms of T/W which is unrealistic and out of bounds for any air-breathing propulsion plant. This is due to the use of a reference MTOW mass for all flight phase and, notably, to the normalization at sea level atmospheric conditions (i.e. it is not a physical condition, rather a problem of chart setting). On the contrary, since the landing requirement is computed in the same way, the value of W/S is consistent with the MMC approach (the subsonic condition is the most demanding one for the determination of wing surface).

The results of the application of the methodology to the considered case study are reported in Table V.

Table V: Results of MMC approach for STRATOFly MR3 case study

Parameter	Value	Unit of Measure
Required Wing surface	1117	m^2
MTOW	369886	kg
OEW	219146	kg
Fuel Capacity	150740	kg
Required ATR engines thrust @ sea level (total)	2842	kN
Required ATR engine thrust @ BOC supersonic (total)	2428	kN
Required DMR engine thrust @ BOC hypersonic	1067	kN
Required DMR engine thrust @ hypersonic cruise level	828	kN

If compared to the values initially assumed within the STRATOFly project for the MR3 vehicle (Table I), some differences can be noted. Particularly, fuel consumption appears here underestimated, whilst the OEW is higher than the reference value. In fact, fuel quantity computation is performed through averaged correlations for cruise and climb phases only (a residual margin is applied to take into account reserves and take-off), being thus simplified. Moreover, OEW is estimated starting from the wing area, resulting from the matching requirements and making benefit of semi-empirical and statistical correlations as shown in [7] and [10]. Differently from conventional aircraft, for which well-established and reliable conceptual design algorithms exist for traditional configurations, the identification of engineering laws describing the architecture of high-speed aircraft is more

difficult, since, in general, a reference configuration is difficult to find and each project is characterized by very peculiar features. OEW is thus a specific characteristic of each aircraft, for which only a high-level value can be determined. However, even if the limitations of the approach are still visible, the main results obtained appear in line with conceptual design reliability boundaries, typically considering margins of about +/- 20% [3] on main design variables. Thrust levels are also in line with the expectation.

5. Conclusions and future works

The paper presents an upgraded mathematical model for the generation of Matching Chart (MC) to widen its range of application to high-speed transportation systems. The diagram traditionally allows the identification of feasible design space (in terms of take-off mass, required thrust and wing surface) that might change depending on the specific flight phases to be faced by the vehicle. Differences with conventional aircraft design have been highlighted and an alternative approach to hypersonic vehicles design, based on Multiple Matching Charts (MMC), has been presented. As example, the case study of STRATOFLY MR3 vehicle is proposed to validate the methodology for the identification of a global design point for a Mach 8 hypersonic cruiser aimed at performing civil passengers transportation. This vehicle configuration is currently under investigation within the H2020 STRATOFLY Project funded by the European Commission. In particular, the application of the methodology to the selected case-study has demonstrated the possibility of determining the global design point for the reference vehicle as well as local design points for the different flight regimes in terms of Thrust-to-Weight ratio (T/W) and Wing Loading (W/S). Moreover, the identified global design point has proved that aero-propulsive balance at hypersonic speed may be critical, since the Dual Mode Ramjet (DMR) of the vehicle may be unable to provide the required level of thrust. A discussion about the inclusion of other kind of requirements, not directly related to aircraft performance, has been carried out, with special attention to the impact of additional statements on design space. Some differences can be highlighted between reference data and results of the method, especially for what concerns aircraft configuration assessment and mass estimation, even if the overall outcome of the analysis is within the limits of application of conceptual design techniques. The integration of the MMC methodology into a complete conceptual design workflow specific for hypersonic vehicle is actually planned as future work. As part of this challenge, several improvements concerning the models used to estimate mass and performance of the vehicles shall be carefully assessed to verify the correctness and robustness of final results. Moreover, to improve the overall effectiveness of the methodology, the design process shall be tested onto other case studies, to assess the confidence level of the results and to ultimately introduce upgrades within the iteration cycle.

Acknowledgment

This project has received funding from the European Union's Horizon 2020 research and innovation programme under grant agreement No 769246 within the Stratospheric Flying Opportunities for High-Speed Propulsion Concepts (STRATOFLY) Project.

References

- [1] J. Roskam, "Airplane Design Part I: Preliminary Sizing of Airplanes (2nd Edition)", DARcorporation, Lawrence, KS, 2003.
- [2] L.R. Jenkinson, P. Simpkin, D. Rhodes (1999) "Civil Jet Aircraft Design", Arnold, London, 1999.
- [3] D.P. Raymer (1992), "Aircraft Design: a Conceptual Approach", AIAA, Washington D.C., 1992.
- [4] R. Fusaro, D. Ferretto, N. Viola, "MBSE approach to support and formalize Mission Alternatives generation and selection processes for hypersonic and suborbital transportation systems", Proc. Of ISEE 2017 – 2017 IEEE International Symposium on Systems Engineering, Vienna, Austria, 2017.
- [5] L.K. Loftin Jr., "Subsonic Aircraft: Evolution and the Matching of Size to Performance", NASA Reference Publication 1060, Nasa Langley Research Center, Hampton, Virginia 1980.
- [6] M. Fioriti, "Adaptable conceptual aircraft design model", Advances in Aircraft and Spacecraft Science, Vol 1. No.1 043-067, 2014.
- [7] B. Chudoba, G. Coleman, A. Oza, L. Gonzalez, P. Czysz, "Solution-space Screening of a Hypersonic Endurance Demonstrator", NASA/CR-2012-217774, NASA Langley Research Center, Hampton, Virginia, 2012.
- [8] A. Ingenito, S. Gulli, C. Bruno, G. Colemann, B. Chudoba, P.A. Czysz, (2011) "Sizing of a Fully Integrated Hypersonic Commercial Airliner", Journal of Aircraft, Vol. 48, No.6, November-December, 2011.
- [9] N. Viola et al., "Main Challenges and Goals of the H2020 STRATOFLY Project", 1st International Conference on Flight Vehicles, Aerothermodynamics and Re-entry Missions & Engineering, Monopoli, Italy, 2019.
- [10] W. E. Hammond, "Design Methodologies for Space Transportation Systems", AIAA Educational Series, Reston, VA (USA), 2001.

- [11] European Aviation Safety Agency (EASA), “Certification specifications and acceptable means of compliance for large aeroplanes CS-25”, Amendment 22, 2018.
- [12] E. H. Hirschel, “Basics of Aerothermodynamics”, Progress in Astronautics and Aeronautics, AIAA, Reston, Va., vol. 204. Springer, Heidelberg, 2004.
- [13] E. H. Hirschel., C. Weiland, “Selected Aero-Thermodynamic Design Problems of Hypersonic Flight Vehicles”, AIAA, Springer, Berlin, 2009.
- [14] R. Fusaro, D. Ferretto, V. Vercella, N. Viola, J. Steelant, V. Fernandez Villace: Life cycle cost estimation methodology for hypersonic transportation systems. Proceedings of the 31st Congress of the International Council of the Aeronautical Sciences, Belo Horizonte, Brazil, 2018.
- [15] V. Vercella, D. Ferretto, R. Fusaro, N. Viola, J. Steelant, V. Fernandez Villace, “Towards future LH2 productive scenarios: economic assessment and environmental effects on hypersonic transportation systems”, 1st Conference on High-speed vehicle science and technology (HiSST), Moscow, Russia, 2018.
- [16] J. Steelant, “Achievements obtained on aero-thermal loaded materials for high-speed atmospheric vehicles within ATLLAS. 16th AIAA International Space Planes and Hypersonic and Technologies Conference. Bremen, Germany, 2009.
- [17] Steelant, J., Varvill, R., Defoort, S., Hannemann, K., Marini, M.: “Achievements Obtained for Sustained Hypersonic Flight within the LAPCAT-II Project”, 20th AIAA International Space Planes and Hypersonic Systems and Technologies Conference, Glasgow, Scotland, 2015.
- [18] E. Blanvillain, E. Gallic, “HIKARI: Paving the way towards high speed air transport”, 20th AIAA International Space Planes and Hypersonic and Technologies Conference. Glasgow, Scotland, 2015.
- [19] J. Steelant et al., “Conceptual Design of the High-Speed Propelled Experimental Flight Test Vehicle HEXAFLY”, 20th AIAA International Space Planes and Hypersonic Systems and Technologies Conference, Glasgow, Scotland, 2015.
- [20] N. Favaloro et al. “Design analysis of the high-speed experimental flight test vehicle HEXAFLY International”, 20th AIAA International Space Planes and Hypersonic Systems and Technologies Conference, Glasgow, Scotland, 2015.
- [21] J. Steelant, T. Langener, (2014) “The LAPCAT MR-2 Hypersonic Cruiser Concept” in 29th Congress of the International Council of the Aeronautical Sciences, St. Petersburg, Russia, 2014.
- [22] A. C. Ispir, B. Saracoglu, P. Goncalves, “Assessment of Combustion Models for thermodynamic modeling of the engines for hypersonic propulsion”, 1st International Conference on Flight Vehicles, Aerothermodynamics and Re-entry Missions & Engineering, Monopoli, Italy, 2019.